Food and Chemical Toxicology 131 (2019) 110552

Contents lists available at ScienceDirect

Food and Chemical Toxicology

journal homepage: www.elsevier.com/locate/foodchemtox

Di-(2-ethylhexyl)-phthalate induces apoptosis via the PPARγ/PTEN/AKT pathway in differentiated human embryonic stem cells

Haiqin Fang[a,b,*,1], Weiting Fang[c,1], Hanwen Cao[a,1], Sha Luo[d], Jingdong Cong[e], Sana Liu[a], Feng Pan[a], Xudong Jia[a,**]

[a] China National Center for Food Safety Risk Assessment, Beijing, 100021, China
[b] The Key Laboratory of Environmental Pollution Monitoring and Disease Control, Ministry of Education, Guizhou Medical University, Guiyang, 550025, China
[c] Affiliated Provincial Hospital of Anhui Medical University & The First Affiliated Hospital of USTC, Division of Life Sciences and Medicine, University of Science and Technology of China. Anhui, 230001, China
[d] Institute of Non-Communicable Diseases Control and Prevention, Tianjin Centers for Disease Control and Prevention, Tianjin, 300011, China
[e] Ziguang Experimental School, WEH, Shandong, 264411, China

ARTICLE INFO

Keywords:
DEHP
hESC
Embryotoxicity
PPARγ receptor
PPARγ/PTEN/AKT signaling pathway

ABSTRACT

[Objective]: Di(2-ethylhexyl) phthalate (DEHP), a widely used plasticizer, may act as an endocrine disruptor and cause developmental toxicity. Differentiated human embryonic stem cells (hESCs) were used to investigate the underlying mechanism of the embryotoxicity induced by DEHP.

[Materials and Methods] H9-hESCs were treated with DEHP at different concentrations for 10 days, and the cytotoxicity of DEHP on cell proliferation was determined using a cell-microelectronic sensing technique (Real-Time Cellular Analysis: RTCA). Based on the 50% inhibitory proliferation concentration (IC_{50}), differentiated H9-hESCs were treated with DEHP at 0, 50, 100, and 200 μg/ml for 120 h, followed by measurement of its toxic effects on the transcriptome by mRNA microarray and QuantiGene Plex (QGP). Proteins were detected by the iTRAQ-based proteomics method and the proteins related to the PPARγ/PTEN/Akt pathways were measured by western blotting. The progression of the cell cycle and apoptosis were characterized using flow cytometry (FCM). In other experiments, hESCs were pre-treated with GW9662 (20 μM), a specific PPARγ inhibitor, for 30 min, followed by exposure to GW9662 (20 μM) and DEHP (200 μg/ml) for 120 h to observe the underlying mechanism of DEHP's embryotoxicity.

[Results]: DEHP inhibited H9-hESC cell proliferation in a dose-dependent manner, with an IC_{50} of 165.78 μg/ml. FCM results showed that DEHP could markedly induce cell cycle arrest and increase apoptosis. Gene microarray and QPG array analyses indicated that the peroxisome proliferator-activated receptor γ (PPARγ) was an apparent target for DEHP. We further demonstrated that DEHP could activate the PPARγ and upregulate the expression of PTEN downstream genes, and then play a negative role in the AKT signaling pathway. Cells pretreated with PPARγ inhibitor, GW9662, were shown to restore the effect of DEHP on the PPARγ/PTEN/AKT signaling pathway, and induce the recovery of cell cycle arrest and apoptosis.

[Conclusion]: DEHP inhibited cell proliferation, promoted cell cycle arrest, and induced apoptosis through the PPARγ/PTEN/AKT signaling pathway in differentiated human embryonic stem cells. It suggested that DEHP exposure possibly cause reproductive or developmental toxicity in humans through the PPARγ signaling pathway.

1. Introduction

DEHP is a widely used plasticizer and ubiquitous environmental contaminant. Leaching, migration, and evaporation of phthalates (Arvanitoyannis and Bosnea, 2004; Inoue et al., 2005) into liquid and solid foods result in human exposure through ingestion, inhalation, and dermal contact (Fang et al., 2017). Among these three pathways, ingestion is considered to be the most common pathway for exposure to

* Corresponding author.China National Center for Food Safety Risk Assessment, Beijing, 100021, China.
** Corresponding author.
E-mail addresses: fanghaiqin@cfsa.net.cn (H. Fang), jiaxudong@cfsa.net.cn (X. Jia).
[1] These authors contributed equally to this work.

https://doi.org/10.1016/j.fct.2019.05.060
Received 11 November 2018; Received in revised form 23 May 2019; Accepted 31 May 2019
Available online 01 June 2019
0278-6915/

phthalate plasticizers. The exposure can be lifelong and represents a major health risk, particularly to vulnerable groups such as infants, pregnant women, and the elderly (Marsee et al., 2006; Swan, 2008).

Results from toxicological animal studies have indicated that exposure to phthalate plasticizers is associated with severe developmental and reproductive toxicities (Duty et al., 2005; Latini, 2005; Singh and Li, 2011). For example, exposure to DEHP in pregnant rats during pregnancy can lead to abnormalities such as exophthalmos, dew, tail, blood vessel, and skeletal abnormalities. DEHP intrauterine exposure can also cause genital malformations in male offspring, such as prostatic malformations, hypospadias, cryptorchidism, and anal–genital distance shortening. DEHP is an established reproductive and developmental toxicant in rodents; however, the pathological consequences and underlying mechanism of exposure to it in humans are unclear.

DEHP, as an endocrine disruptor, is thought to exert its effects through binding to nuclear hormone receptors (Casals-Casas and Desvergne, 2011). Much of the current knowledge about *in utero* and postnatal exposure to endocrine disruptors has been focused on development, particularly in reproductive systems (Barakat et al., 2017; Cardoso et al., 2017). The nuclear receptor PPARγ has been identified as a specific molecular target in which MEHP, the monoester metabolite of DEHP, functions as an agonist in *in vitro* assays (Casals-Casas et al., 2008; Feige et al., 2007). *In vitro* and in vivo experiments have also demonstrated that DEHP stimulates the activation of PPARγ and leads to the production of oxidative stress and downregulated expression of insulin receptor and GLUT4 proteins, disrupting the insulin signaling pathway in the liver of SD rats and L02 cells (Hunt et al., 2017; Zhang et al., 2017; Rowdhwal and Chen, 2018). However, the potential impact of DEHP on PPARγ in reproductive and developmental toxicity remains understudied.

hESCs are healthy immortalized cells derived from undifferentiated cells in the blastocysts. They can be propagated for long periods in vitro under suitable conditions. hESCs can simultaneously differentiate into different types of cell in the three germ layers, forming a variety of normal adult cells (Jensen et al., 2009; Pal et al., 2011). This differentiation process simulates the early development of human embryos. Moreover, the hESC model is an excellent tool to observe change at the cellular level and determine the role of specific pathways by positive or negative interaction. Considering the unparalleled superiority of hESCs compared with traditional animal experiments or other experimental models in vitro, we used differentiated hESCs to investigate the mechanism underlying DEHP's embryonic toxicity in the study presented here.

In our previous study, we established a hESC test (hEST) model according to the protocol of the Embryonic Stem Cell Test (Scholz and Spielman, 2000; Genschow et al., 2004) and used this model to evaluate diethylhexyl phthalate (DEHP) as a chemical with weak embryotoxicity (Luo et al., 2016).

2. Material and methods

2.1. Reagents

Di-(2-ethylhexyl)-phthalate (DEHP) (purity > 99.0%) was purchased from Sigma (Sigma-Aldrich, Italy), prepared as a nanoemulsion (NE) stock solution of 100 mg/ml, and diluted to final concentrations in all experiments with cell culture medium. mTeSR-1, Releasal Enzyme-free human ES and iPS cell selection and passaging reagent, Rho-associated coiled-coil containing protein kinase (ROCK) inhibitor Y-27632, Accutase™ cell detachment solution, and Aggrewell™ plates were purchased from Stemcell Technologies (Vancouver, Canada). β-Mercaptoethanol was purchased from Sigma-Aldrich (Munich, Germany). Cell counting kit (CCK-8) was purchased from Dojindo Laboratories (Tokyo, Japan). Fetal bovine serum (FBS), DMEM, non-essential amino acids, and L-glutamine were purchased from Gibco BRL (Germany). Primary antibodies against PPARγ, PTEN, phospho-Akt (Ser473), phospho-mdm2 (Ser166), phospho-p53 (Ser15), phospho-Bad (Ser136), Bax, Bcl-2, and phospho-cdc2, as well as HRP-labeled secondary antibodies, were purchased from Cell Signaling Technology (Danvers, MA, USA). The PPARγ-specific antagonist, GW9662, was obtained from Selleck Chemicals (Houston, TX, USA). All other reagents were of analytical grade.

2.2. DEHP nanoemulsion preparation

DEHP nanoemulsions (NEs) were prepared using a 5% w/v bovine serum albumin (BSA) water solution with 0.1% β-mercaptoethanol (Sigma-Aldrich, Italy), 1 ml of DEHP (1.0 g/ml) resolved with 1 ml of ethanol, and 8 ml of 5% BSA water solution. The mixtures were treated with ultrasound at 20 kHz at the air–water interface, using a Sonics and Materials ultrasound generator (Branson) with a 3-mm-diameter horn at an applied acoustic power of 160 Wcm^{-2} for 60 s. After sonication, the samples were incubated with gentle shaking at 4 °C for about 48 h. Milky suspensions containing the DEHP-NEs were recovered, transferred to a new tube, sterilized by 0.22-μm filtration, characterized by a nanoparticle size analyzer and for zeta potential with dynamic light scattering (DLS), and finally stored at −80 °C.

2.3. hESC culture

hESCs (H9 cell line; WiCell, Madison, WI; passages 35–40) were maintained under feeder-independent culture conditions, using BD Matrigel human ESC-qualified Matrix (BD Biosciences, San Jose, CA), and grown in mTeSR-1 (Stemcell Technologies, Vancouver, Canada) at 37 °C and 5% CO_2. Cell cultures were maintained and expanded in accordance with the manufacturer's protocol. Cultures of differentiating human ES cells were established by the formation of embryo bodies (EBs) using an Aggrewell™ plate, as previously reported (Luo et al., 2016).

2.4. hESC cell proliferation

DEHP cytotoxicity in hESCs (IC_{50}H9) was measured by CCK-8 method as previously reported (Luo et al., 2016; Fang et al., 2018) and the RTCA System (ACEA Biosciences, San Diego, CA) (Kustermann et al., 2013). For RTCA, 1 h before the experiment, 150 μL of the medium was added to each well and the baseline data were recorded. Following background measurement, 300 μL of medium containing 1500 cells in suspension was seeded on the E-Plate™ in each well. DEHP was immediately added at different concentrations (0, 12.5, 25, 50, 100, 200, 400, or 800 μg/ml), followed by incubation at room temperature for 1 h and placement on the device station, with final incubation at 37 °C with 5% CO_2. The cells were allowed to equilibrate for 2–4 h, with constant impedance monitoring every 30 min for the remaining time (> 120 h). The medium was changed every day. Data were normalized by comparison with control cultures, which were considered to reflect 100% cell survival.

2.5. hESC cell cycle and apoptosis

EBs generated by H9-hESCs were seeded in six-well plates with 10 EBs/well and treated with DEHP (0, 50, 100, or 200 μg/ml) in differentiation medium (15% FBS, 83% DMEM, 1% NEAA, and 1% L-glutamine) for 120 h. The medium was changed every day. For cell cycle analysis, cells were collected and fixed with 70% ethanol at 4 °C for 4 h. After washing with cold PBS, cells were resuspended with 500 μl of propidium iodide (PI) (Life Technology, Oregon, USA) and incubated at 37 °C in the dark for 20 min, followed by analysis with a FACS Calibur flow cytometer. Apoptosis of cells was determined with an Annexin V-FITC Apoptosis Detection Kit (BD Biosciences, San Jose, CA, USA), in accordance with the manufacturer's instructions.

2.6. Transcriptome microarray

Differentiated hESCs were treated with DEHP (100 μg/ml) for 120 h. Total RNA was extracted from hESCs (DEHP groups and the control) using Trizol reagent (Invitrogen, Carlsbad, CA, USA), and purified with Agencourt Ampure magnetic beads (APN 000132; Beckman Coulter). The GeneChips of Human Transcriptome Array 2.0 (Affymetrix, USA) were used for whole-transcript expression profiling. Genes with threshold values of fold change ≥ 2.0 or ≤ -2.0 were designated as being differentially expressed. The Database for Annotation, Visualization, and Integrated Discovery (DAVID) was used to determine pathways and processes of major biological significance based on the Gene Ontology (GO) annotation function and Kyoto Encyclopedia of Genes and Genomes (KEGG) pathway function.

2.7. QGP assay

The QGP assay was then carried out in accordance with the manufacturer's directions using 500 ng of purified RNA per well, with two replicates per sample. Probes against genes were designed by Affymetrix. The incubations were carried out in a VorTemp shaking incubator (LabNet, Edison, NJ), and washes were accomplished with the aid of a magnetic plate holder (Invitrogen, Carlsbad, CA). Assay plates were then stored at 4 °C overnight, brought up to room temperature, and analyzed on a MagPix reader (Luminex, Austin, TX). Median fluorescent intensity (MFI) readings were recorded for all samples. A baseline of twice the limit of detection (as recommended by the manufacturer) was used as the minimum signal allowed for the genes analyzed. Expression of genes of interest was normalized by dividing by three reference genes (TBP, TRFC, TXNRD1), and the geometric mean of three genes was calculated by GEOMEAN. For some selected genes, real-time polymerase chain reactions (real-time PCR) was used to identify.

2.8. iTRAQ method

Quan-titative proteomic analysis was performed according to the methodology described in previous studies (Fu et al., 2013; Chen et al., 2017; Verano-Braga et al., 2014; Doering et al., 2016), with some modifications. Total proteins were extracted from samples using 400 μL of lysate (7 M urea, 2 M thiourea, 0.1% PMSF, a protease inhibitor, 65 mM DTT) to 10^6 cells, and the protein concentrations were determined using the Bradford colorimetric method.

From each sample, 100 μg of protein was reduced, alkylated, and digested prior to labeling with iTRAQ reagent, in accordance with the manufacturer's instructions (AB Sciex, Framingham, MA). Digested proteins prepared from each sample were labeled with iTRAQ reagent, and peptides were subjected to a trap and reverse-phase (RP) analytical column by using a gradient of 0%–50% solvent B in solvent A over 140 min (solvent A: 0.1% trifluoroacetic acid [TFA] and 2% acetonitrile; solvent B: 0.1% TFA and 70% acetonitrile). The RP analytical column eluent was spotted onto a MALDI sample plate using a DNA Direct Nano-flow LC/MALDI system (KYA Tech, Tokyo, Japan) and analyzed by a 4800 mass spectrometer (AB Sciex, Framingham, MA). Relative protein abundance was determined using MS/MS scans of the iTRAQ-labeled peptides. iTRAQ-labeled peptides were fragmented under collision-induced dissociation conditions to generate fragment ions that provided sequence information for the peptide and reporter ions. Thus, the identity of the protein from the analyzed peptide could be confirmed, and the ratios of the peak areas of iTRAQ reporter ions were used to compare the relative abundance of the protein identified in the sample. Proteins with threshold values of fold change ≥ 1.5 or ≤ -1.5 were designated as being differentially expressed. ProteinPilot v4.0 (AB Sciex, Framingham, MA) was used for data analysis using NCBI and SWISS-PROT databases.

2.9. Western blotting

Homogenated proteins (10–40 μg) from differentiated hESC lysate were resolved on SDS-polyacrylamide gels (NuPAGE; Invitrogen, Carlsbad, CA, USA) and electrophoretically transferred onto polyvinylidene fluoride membranes. After blocking with 5% skim milk, the membranes were incubated with specific primary antibodies and then corresponding HRP-labeled secondary antibodies. Membranes were developed with West Femto Chemiluminescent Substrate (Thermo, Rockford, IL, USA) and the images were captured with the Syngene GeneGnome XRQ system (BioTek, Hong Kong, China). The relative expression of proteins was quantified by band area and density with Image J software and normalized with β-actin. In some experiments, cell lysates of hESCs were collected for PathScan Akt Signaling Array assay, in accordance with the manufacturer's instructions (Cell Signaling Technology Inc., Danvers, MA, USA).

2.10. Statistical analysis

Data are expressed as mean ± SD and were analyzed by one-way ANOVA, followed by Bonferroni, using SPSS 11.5 statistical software (Ranstam, 2016). The level of significance was set at $P < 0.05$.

3. Results

3.1. Synthesis and characterization of DEHP-NEs

DEHP-NEs were prepared by sonication of a 5% w/v bovine serum albumin (BSA) solution. After dilution with distilled de-ionized water, the DEHP-NEs (0.25 mg/ml) were characterized by DLS. The size

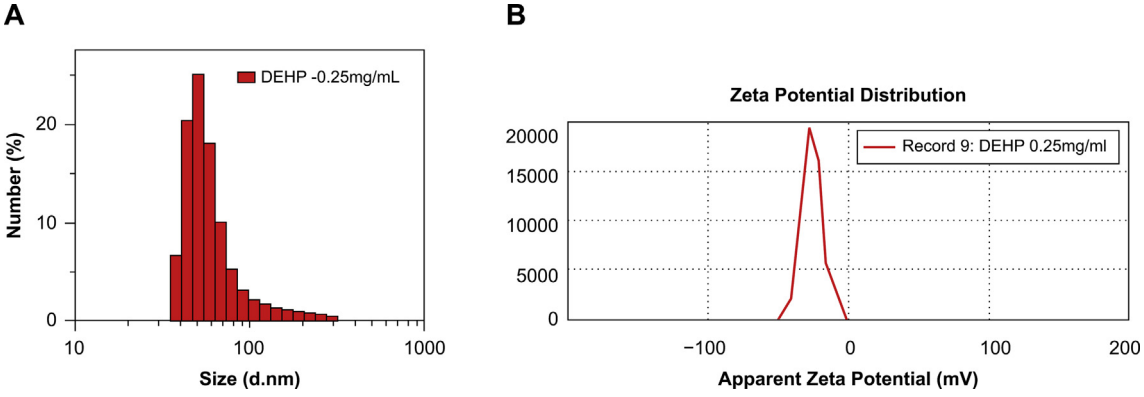

Fig. 1. DLS analysis of DEHP-NEs. Mean diameter of the DEHP-NE (0.25 mg/ml) spheres was 0.06–0.08 μm (Fig. 1A) and stable station with zeta potential at 11–18 mV (Fig. 1B).

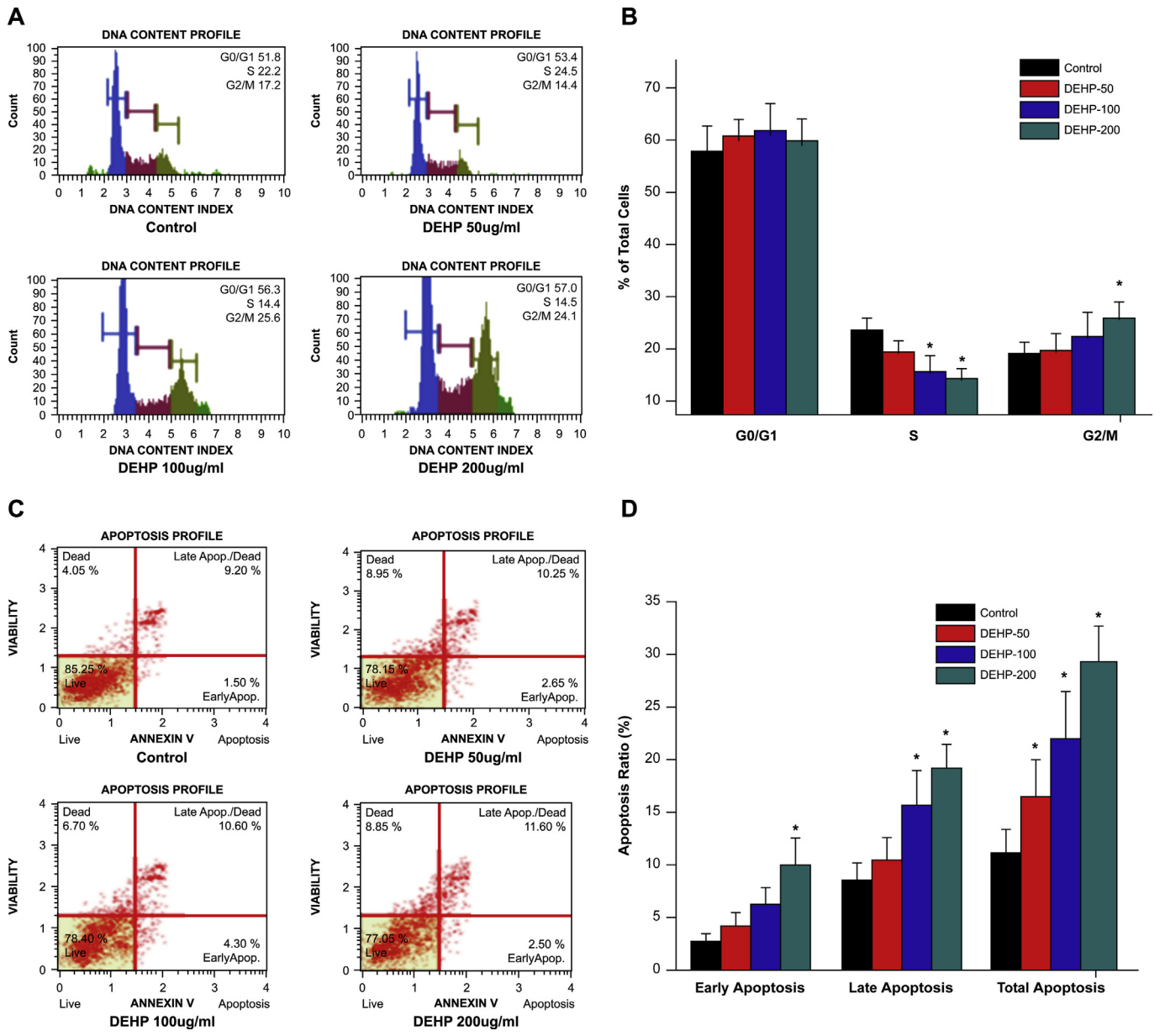

Fig. 2. DEHP induced cell cycle arrest and apoptosis in differentiated hESCs. Cell cycle arrest, including a decrease in S-phase cells and an increase in G_0/G_1-phase cells, was shown to occur in a dose-dependent manner (Fig. 2A and B). The apoptosis induced by DEHP was observed upon DEHP exposure at different concentrations, especially at 200 μg/ml (Fig. 2C and D). Values were presented as the mean ± standard deviation (SD). *, $p < 0.05$ compared with the control group.

distribution of DEHP-NEs is presented in Fig. 1. The mean diameter of the DEHP-NE spheres was 0.06–0.08 μm (Fig. 1A) and stable station with zeta potential of 11–18 mV (Fig. 1B).

3.2. Cell culture

As shown in SI-1, the undifferentiated hESC-H9 cells (Figure SI-1A) showed typical clonal nest-like shape, with smooth and clear boundaries. hESC EBs were generated in the AggrewellTM plate for 2 days (Figure SI–1B) according to STEMCELL's AggrewellTM EB plate standard operating procedure. After suspending hEBS (Figure SI–1C) in low-attached dishes for 3 days (for hEBs), EBs were planted on 0.1% gelatin-coated 24-well plates (Figure SI-1D) and differentiated spontaneously into multiple types of cells on day 5 + 5 (Figure SC-1E).

3.3. DEHP induced cell cycle arrest and apoptosis in hESCs

The effects of DEHP on the cell cycle involved the proportion of S-phase cells gradually decreasing and that of G_0/G_1-phase cells steadily increasing upon its addition at 100 or 200 μg/ml, in a dose-dependent manner (Fig. 2A and B). This suggested that DEHP induces cell cycle arrest in differentiated hESCs.

Moreover, a significant change of apoptosis due to DEHP was observed upon exposure to it at different concentrations, especially 200 μg/ml (Fig. 2C and D). These findings indicated that DEHP inhibited cell proliferation in the differentiated hESCs by inducing cell cycle arrest as well as by promoting apoptosis.

3.4. DEHP inhibited proliferation of hESCs by PPARγ

As shown in Fig. 3A and B, DEHP inhibited hESC proliferation and

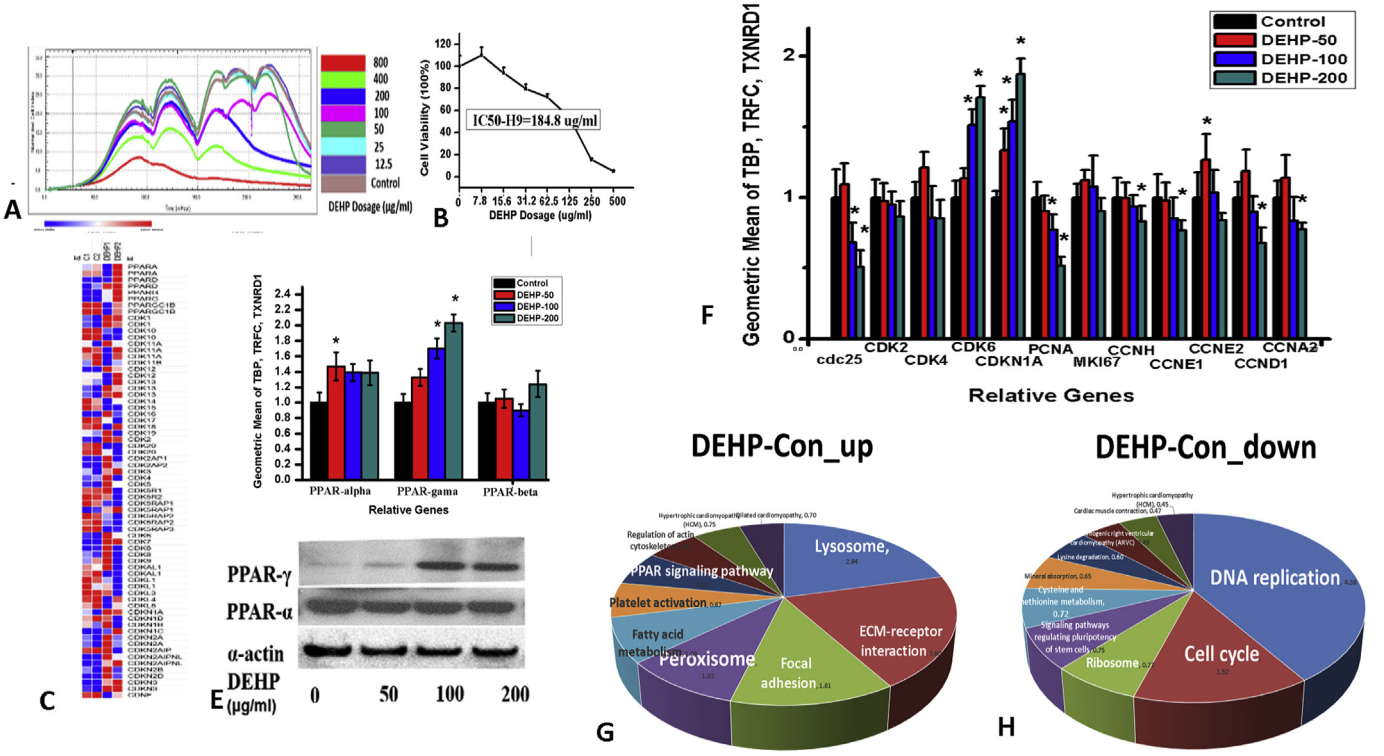

Fig. 3. DEHP inhibited cell proliferation, activated PPARγ, and affected genes related to the cell cycle. DEHP inhibited hESC proliferation and viability in a dose-dependent manner (Fig. 3A and B). Compared with the control, the transcriptome profiling showed that PPARγ was significantly upregulated in hESCs treated with DEHP at 100 μg/ml (Fig. 3C). The results of QGP (Fig. 3D) and western blotting (Fig. 3E) also showed that DEHP increased PPARγ expression in a dose-dependent manner. The genes related to cell proliferation were measured by QGP (Fig. 3F). The KEGG pathway analysis based on iTRAQ results showed that the most significant decreases were related to DNA replication and the cell cycle and that there were marked increases for both the PPAR signaling pathway and the peroxisome pathway in the DEHP-treated group, when compared with normally differentiated hESCs (Fig. 3G and H). Values were presented as the mean ± SD. *, $p < 0.05$ compared with the control group.

viability in a dose-dependent manner, and the IC_{50}H9 of DEHP was determined to be 165.7 μg/ml by RCTA (3A) and 148.8 μg/ml by CCK-8 method (3B). To elucidate the mechanisms underlying the hESC growth inhibition by DEHP, a microarray analysis was carried out, and 1899 genes down-regulated and 1177 genes up-regulated were shown in the transcriptome profiling of differentiated hESCs treated with DEHP.

Previous studies reported that PPARs were DEHP target binding sites (Zhang et al., 2017). Based on the differentially expressed genes as revealed in the transcriptome microarray, including PPAR family genes (PPARα, PPARβ, and PPARγ), PPARγ was identified as being significantly upregulated in hESCs treated with DEHP at 100 μg/ml, compared with the level in the control (Fig. 3C, SI-2). The results of QGP and real-time PCR also showed that DEHP increased PPARγ gene expression in a dose-dependent manner (Fig. 3D, SI-4). Moreover, the protein expression analysis confirmed that DEHP was an agonist of PPARγ (Fig. 3E); however, there were no significant changes in the expression of PPARα and PPARβ genes, and PPARα protein. It was thus confirmed that PPARγ was the target receptor for DEHP in differentiated hESCs.

We further investigated the impact of DEHP on the expression of genes for cell proliferation, survival, and apoptosis in hESCs. The results of microarray and QPG and real-time PCR assay analyses showed that the expression of cyclin A, CDK2, and CDK4 decreased, while that of CDK6 increased significantly (Fig. 3F, SI-4). At the same time, CDK inhibitors, including CDKN1A and CDKN1D, were dose-dependently increased by DEHP (Fig. 3F).

In total, 5982 proteins were identified of which 5963 proteins could be quantified by iTRAQ quantitatively analyse. Among those quantified, 106 and 134 proteins were up- and down-regulated, respectively (Tables SI–3). Based on the iTRAQ results, compared with normally differentiated hESCs, the KEGG pathway analysis showed that the most significant decreases occurred for DNA replication (41%) and cell cycle (14%) in the DEHP-treated group. Moreover, marked increases for both the PPAR signaling pathway (6%) and the peroxisome pathway (9%) were also observed in this group (Figs. 3G, 3H, SI-3).

3.5. DEHP inhibited ESC proliferation by targeting the Akt signaling pathway

The expression of the tumor suppressor gene PTEN, which is transcriptionally regulated and activated by PPARγ and acts as a primary negative regulator of PI3K/Akt signaling, was also increased by DEHP (Figure SI-5A, 4B). The PI3K-Akt pathway is known to play an essential role in regulating various cellular functions (including metabolism, growth, proliferation, survival, transcription, and protein synthesis). Thus, we speculated that Akt signaling could be a potential target for DEHP inhibition of hESC proliferation. Using the Akt Signaling Array assay, we observed that DEHP treatment significantly decreased the phosphorylation of Akt (Ser 473/Thr 308), S6 ribosomal protein (Ser 235/236), and PRAS40 (Thr246), and increased PTEN and 4E-BP1 (Figure SI–5B). This suggests that DEHP significantly attenuated the activation of the Akt signaling pathway during hESC differentiation.

In addition, we further investigated the impact of DEHP on the downstream molecules of Akt that govern cell proliferation, survival, and apoptosis in differentiated hESCs. First, the blockade of Akt activation by DEHP was confirmed at all dose levels (50, 100, and 200 μg/ml) (Figure SI–5C). Akt-mediated phosphorylation of mdm2 at Ser166 was also markedly decreased by DEHP, which inhibited the degradation of the tumor suppressor p53. Moreover, the expression of the CDK inhibitor p21 was dose-dependently restored by DEHP. Inversely, the

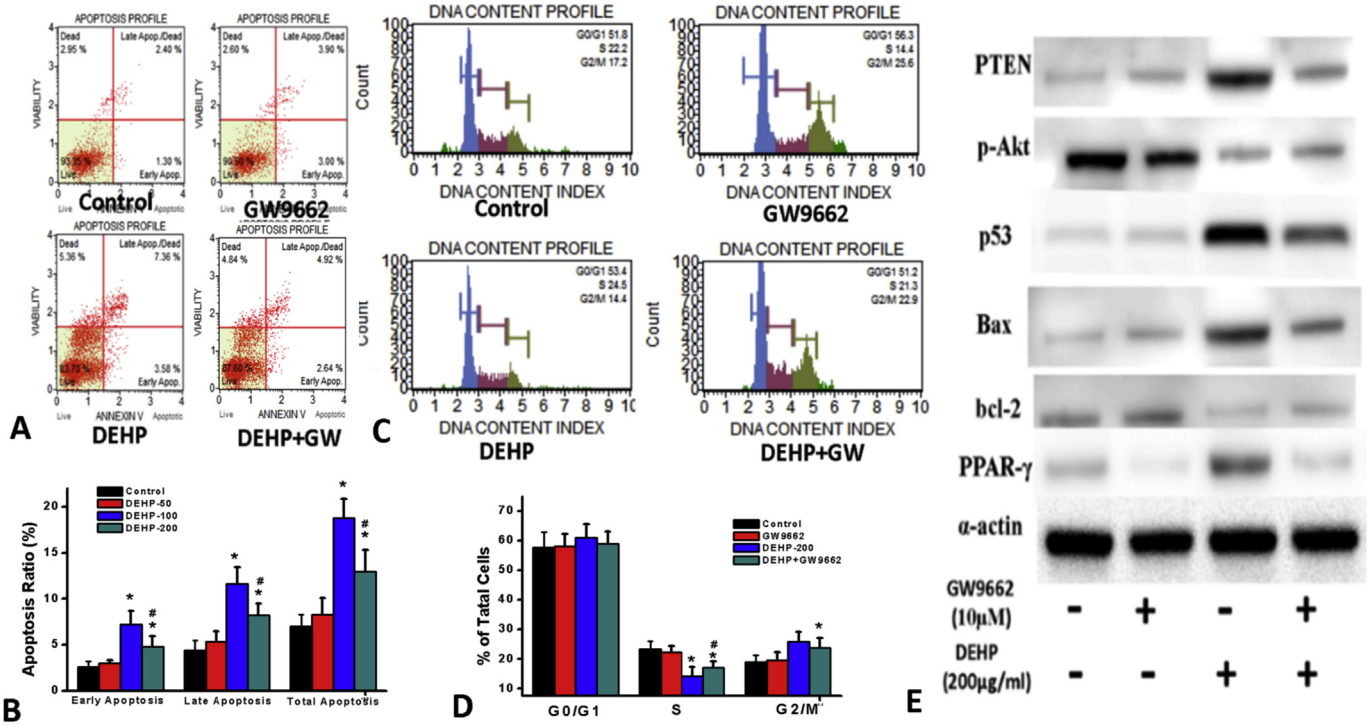

Fig. 4. The effects of DEHP and GW9662 on PPARγ/PTEN/Akt signaling, cell cycle, and apoptosis. Apoptosis (Fig. 4A and B) and the cell cycle (Fig. 4C and D) were measured using FCM treated with DEHP (200 μg/ml) and GW9662 (20 μM) for 120 h. Protein expression of p-Akt, p53, p21, Bax, and bcl-2 in hESCs treated with DEHP (200 μg/ml) and GW9662 (20 μM) for 120 h was measured by western blotting (Fig. 4E). Values were presented as the mean ± SD. *, $p < 0.05$ compared with the control group.#, $p < 0.05$ DEHP + GW9662 group compared with the DEHP group.

phosphorylation of cdc2, which promotes cell cycle transition, was suppressed by DEHP, which is in line with the effect of DEHP on cell cycle arrest. Finally, the expression of the pro-apoptotic protein Bax was increased and that of pro-survival bcl-2 was consistently decreased (Figure SI–5C). Collectively, these findings suggest that DEHP inhibits differentiated hESC proliferation by attenuating Akt activation, resulting in the subsequent suppression of cell growth and survival, and the promotion of apoptosis.

To confirm our hypothesis, the specific antagonist of PPARγ, GW9662, was used in differentiated hESCs. The apoptosis (Fig. 4A and B) and cell cycle arrest (Fig. 4C and D) induced by DEHP were recovered from by this inhibitor. PPARγ activation by DEHP significantly inhibited the phosphorylation of Akt, whereas the downstream p53, p21, and Bax were instead increased (Fig. 4E). In contrast, the PPARγ inhibitor GW9662 markedly increased the phosphorylation of Akt and its downstream target molecules (p53, p21, Bax, and bcl-2), which was affected by the presence of DEHP (Fig. 4E). Taking these findings together, it is suggested that PPARγ activation plays a critical role in the suppression of the Akt signaling pathway by DEHP.

4. Discussion

Animal experiments have shown that DEHP's embryonic toxicity and teratogenic toxicity exhibit significant dose- and age-dependent characteristics. At the same dose, young animals have been shown to be more sensitive than adults, suggesting that DEHP could act on cell proliferation. Human exposure to DEHP may begin in the womb, where DEHP has been demonstrated to readily cross the placenta and accumulate in the fetus (Lin et al., 2015; Xu et al., 2007). Despite these observations, the productive and developmental effects of DEHP have been examined in only a few animal studies, and the underlying mechanisms remain unclear.

hESCs show unparalleled superiority compared with traditional animal experiments or other experimental models as the differentiation process of hESCs accurately simulates the early development of human embryos (Yu et al., 2013). Based on the concept that the process of EB generation and differentiation from hESCs is an appropriate model to simulate the early developmental process of the human embryo in vitro, we used differentiated EBs to investigate the underlying mechanism of DEHP embryotoxicity.

It should be noted that, in DEPH-treated cell culture medium, it is difficult to maintain cells in a homogeneous and stable state of dispersion since DEHP is oil-soluble. In this study, the critical step to overcoming this difficulty was the preparation of DEHP at the nanoscale with stable zeta potential.

Another crucial point in performing cytotoxicity assays is that it is difficult for human ESCs to survive in a single-cell phase. In the present study, this problem was solved by using Accutase™, which can detach hESCs into single cells, along with the use of the ROCK inhibitor Y-27632 to ensure the survival of single H9 cells on RTCA plates. Y-27632 was shown to increase the survival of cryopreserved single hESCs after thawing (Li et al., 2009) and to improve embryoid body formation using forced-aggregation protocols (Ungrin et al., 2008). The real-time cell electronic sensing system was used by an electronic impedance readout to quantify adherent cell proliferation and noninvasive viability in real time.

The potential health hazards, including embryotoxicity, from exposure to DEHP could be related to its role or that of its metabolites in the trans-activation of PPARs (Xu et al., 2006). PPARs are nuclear steroid receptors that regulate diverse biological processes such as lipid and carbohydrate metabolism, development, differentiation, apoptosis, neoplastic transformation, inflammation, and regeneration (Li and Liu, 2018). PPARγ agonists have been reported to activate phosphatase and tensin homolog deleted on chromosome 10 (PTEN) protein expression (Patel et al., 2001). PTEN is a tumor suppressor protein and inhibits the activation of the PI3K/Akt cascade via dephosphorylation of position 3 phosphates of phosphatidylinositol (3,4,5)-trisphosphate (PIP3) to produce phosphatidylinositol 4,5-bisphosphate (PIP2) (Yousefi et al.,

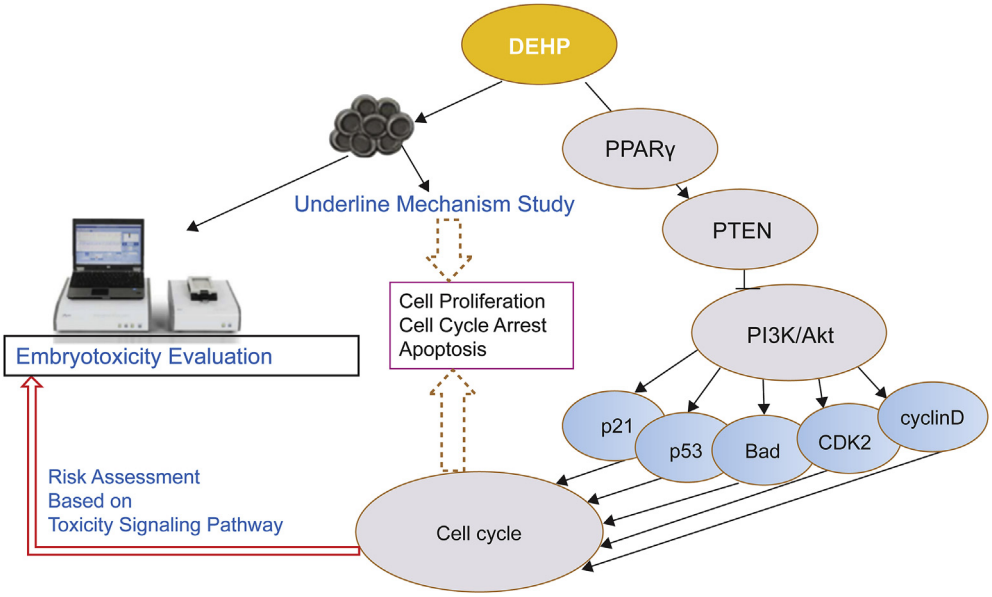

Fig. 5. Working model of DEHP embryotoxicity evaluation and the mechanism by regarding the PPAR/PTEN//AKT pathway.

2017; Schwartz and Shah, 2005). In the present study, the upregulation of PTEN was observed after the activation of PPARγ.

The PTEN/PI3 K/AKT survival pathway has been suggested to play an important role in many aspects of cancer development, such as cell apoptosis, proliferation, migration, and angiogenesis (Carnero et al., 2008; Jiang and Liu, 2008). In our study, the upregulation of PTEN and the downregulation of p-AKT indicated the dysregulation of the PTEN/PI3K/AKT survival pathway in hESCs by DEHP. This inhibitory effect of DEHP on the PTEN/PI3K/AKT survival pathway was confirmed by applying a PPARγ inhibitor. The results indicated that the anti-proliferative effect of DEHP in hESCs was related to the PTEN/PI3K/AKT survival pathway.

The blockage of cell cycle progression usually leads to the apoptosis of cells, which is the form of programmed cell death that governs the cell survival/death balance. In the present study, we found that DEHP significantly induced the apoptosis of hESCs. As reported previously, DEHP exposure induced oxidative stress and DNA damage, which activated the p53-dependent apoptotic pathway in vivo and in vitro (Erkekoglu et al., 2014; Ha et al., 2016). Mdm2, an important negative regulator of p53, was also suppressed by DEHP, which then induced p53-dependent apoptosis via the induction of oxidative stress (Hafsi et al., 2012). In this study, the increase of p53 and decrease of mdm 2 were observed after DEHP exposure in hESCs. Bax and Bcl-2 proteins belong to the Bcl-2 family, and the Bcl-2/Bax ratio is an important index for apoptosis. It was reported that the balance of proapoptotic factors (such as Bad and Bax) and antiapoptotic factors (such as Bcl2) was generally broken by DEHP exposure in ovarian follicular atresia (Hannon et al., 2015). This study showed that DEHP caused marked dysregulation of the ratio of Bcl-2/Bax, which suggested that it promoted the apoptosis of hESCs.

In our experiments, the increase of PPARγ expression induced by DEHP treatment was clearly inhibited by GW9662. Moreover, the activation of p53 and p21 was reversed by GW9662 in response to Akt repression. In addition, the anti-apoptotic protein Bcl-2 and the pro-apoptotic Bax were inversely regulated by DEHP. Collectively, these findings suggest that DEHP inhibits hESC-H9 cell proliferation by attenuating Akt activation, resulting in the subsequent suppression of cell growth and survival, and the promotion of apoptosis.

It was reported that DEHP was present in pregnant women (17 out of 24 subjects) and in cord samples (11 out of 25 subjects). The mean DEHP concentrations in maternal and cord plasmas were 1.15 ± 0.81 and 2.05 ± 1.47 mg/ml, respectively (Latini et al., 2003). It seemed that the range between the DEHP's toxic endpoints in vitro and the exposure in pregnant women's in vivo was a wide margin of safety. Although the significant dose-response relationship can confirm that DEHP has some embryonic developmental toxicity, to extrapolate the risk to human may still have big uncertainty.

In conclusion, the present study demonstrated that DEHP inhibited hESC proliferation, and induced cell cycle arrest and apoptosis via the PPARγ/PTEN/PI3K/AKT survival pathway (Fig. 5). We speculate that this might be the molecular mechanism underlying DEHP-induced embryonic toxicity.

Acknowledgments

This project was supported by State Key R&D Project, No. 2018YFC1603102, the open project of the Key Laboratory of Environmental Pollution Monitoring and Disease Control, Ministry of Education, Guizhou Medical University, China (GMU-2019-HJZ-02), the National Natural Science Foundation of China (No. 81673173), and China Food Safety Talent Competency Development Initiative: CFSA 523 Program.

Appendix A. Supplementary data

Supplementary data to this article can be found online at https://doi.org/10.1016/j.fct.2019.05.060.

References

Arvanitoyannis, I.S., Bosnea, L., 2004. Migration of substances from food packaging materials to foods. Crit. Rev. Food Sci. Nutr. 44 (2), 63–76.
Barakat, R., Lin, P.P., Rattan, S., et al., 2017. Prenatal exposure to DEHP induces premature reproductive senescence in male mice. Toxicol. Sci. 156 (1), 96–108.
Cardoso, A.M., Alves, M.G., Mathur, P.P., et al., 2017. Obesogens and male fertility. Obes. Rev. 18 (1), 109–125.
Carnero, A., Blanco-Aparicio, C., Renner, O., et al., 2008. The PTEN/PI3K/AKT signaling pathway in cancer, therapeutic implications. Curr. Cancer Drug Targets 8 (3), 187–198.
Casals-Casas, C., Desvergne, B., 2011. Endocrine disruptors: from endocrine to metabolic disruption. Annu. Rev. Physiol. 73, 135–162.
Casals-Casas, C., Feige, J.N., Desvergne, B., 2008. Interference of pollutants with PPARs: endocrine disruption meets metabolism. Int. J. Obes. 32 (Suppl. 6), S53–S61.
Chen, L., Hu, Y., He, J., et al., 2017. Responses of the proteome and metabolome in livers of zebrafish exposed chronically to environmentally relevant concentrations of microcystin-LR. Environ. Sci. Technol. 51, 596–607.

Doering, J.A., Tang, S., Peng, H., 2016. High conservation in transcriptomic and proteomic response of white sturgeon to equipotent concentrations of 2,3,7,8-TCDD, PCB 77, and benzo[a]pyrene. Environ. Sci. Technol. 50, 4826–4835.
Duty, S.M., Calafat, A.M., Silva, M.J., et al., 2005. Phthalate exposure and reproductive hormones in adult men. Hum. Reprod. 20 (3), 604–610.
Erkekoglu, P., Zeybek, N.D., Giray, B.K., et al., 2014. The effects of di(2-ethylhexyl) phthalate on rat liver in relation to selenium status. Int. J. Exp. Pathol. 95 (1), 64–77.
Fang, H., Wang, J., Lynch, R.A., 2017. Migration of di(2-ethylhexyl)phthalate (DEHP) and di- n -butylphthalate (DBP) from polypropylene food containers. Food Control 73, 1298–1302.
Fang, H., Zhi, Y., Yu, Z., Lynch, Robert A., Jia, X., 2018. The embryonic toxicity evaluation of deoxynivalenol (DON) by murine embryonic stem cell test and human embryonic stem cell test models. Food Control 86, 234–240.
Feige, J.N., Gelman, L., Rossi, D., et al., 2007. The endocrine disruptor monoethyl-hexyl-phthalate is a selective peroxisome proliferator-activated receptor gamma modulator that promotes adipogenesis. J. Biol. Chem. 282 (26), 19152–19166.
Fu, J., Han, J., Zhou, B.S., et al., 2013. Toxicogenomic responses of zebrafish embryos/larvae to tris(1,3-dichloro-2-propyl) phosphate (TDCPP) reveal possible molecular mechanisms of developmental toxicity. Environ. Sci. Technol. 47, 10574–10582.
Genschow, E., Spielmann, H., Scholz, G., Pohl, I., Seiler, A., Clemann, N., et al., 2004. Validation of the embryonic stem cell test in the international ECVAM validation study on three in vitro embryotoxicity tests. Alternatives to Laboratory Animals 32, 209–244.
Ha, M., Wei, L., Guan, X., et al., 2016. p53-dependent apoptosis contributes to di-(2-ethylhexyl) phthalate-induced hepatotoxicity. Environ. Pollut. 208 (Pt B), 416–425.
Hafsi, S., Pezzino, F.M., Candido, S., et al., 2012. Gene alterations in the PI3K/PTEN/AKT pathway as a mechanism of drug-resistance (review). Int. J. Oncol. 40, 639–644.
Hannon, P.R., Brannick, K.E., Wang, W., et al., 2015. Di(2-ethylhexyl) phthalate inhibits antral follicle growth, induces atresia, and inhibits steroid hormone production in cultured mouse antral follicles. Toxicol. Appl. Pharmacol. 284 (1), 42–53.
Hunt, B.G., Wang, Y.L., Chen, M.S., et al., 2017. Maternal diethylhexyl phthalate exposure affects adiposity and insulin tolerance in offspring in a PCNA-dependent manner. Environ. Res. 159, 588–594.
Inoue, K., Kawaguchi, M., Yamanaka, R., et al., 2005. Evaluation and analysis of exposure levels of di(2-ethylhexyl) phthalate from blood bags. Clin. Chim. Acta 358, 159–166.
Jensen, J., Hyllner, J., Björquist, P., 2009. Human embryonic stem cell technologies and drug discovery. J. Cell. Physiol. 219 (3), 513–519.
Jiang, B.H., Liu, L.Z., 2008. PI3K/PTEN signaling in tumorigenesis and angiogenesis. Biochim. Biophys. Acta 1784 (1), 150–158.
Kustermann, S., Boess, F., Buness, A., Schmitz, M., Watzele, M., Weiser, T., Singer, T., Suter, L., Roth, A., 2013. A label-free, impedance-based real time assay to identify drug-induced toxicities and differentiate cytostatic from cytotoxic effects. Toxicol. Vitro 27 (5), 1589–1595.
Latini, G., 2005. Monitoring phthalate exposure in humans. Clin. Chim. Acta 361, 20–29.
Latini, G., De Felice, C., Presta, G., Del Vecchio, A., Paris, I., Ruggieri, F., Mazzeo, P., 2003. Exposure to Di(2-ethylhexyl)phthalate in humans during pregnancy. A preliminary report. Biol. Neonate 83 (1), 22–24.
Li, J., Liu, Y.P., 2018. The roles of PPARs in human diseases. Nucleos Nucleot. Nucleic Acids 23, 1–22.
Li, X., Krawetz, R., Liu, S., et al., 2009. ROCK inhibitor improves survival of cryopreserved serum/feeder-free single human embryonic stem cells. Hum. Reprod. 24 (3), 580–589.
Lin, H., Yuan, K., Li, L., et al., 2015. Utero exposure to diethylhexyl phthalate affects rat brain development: a behavioral and genomic approach. Int. J. Environ. Res. Public Health 12 (11), 13696–13710.
Luo, S., Fang, H.Q., Yang, H., et al., 2016. Comparison of embryotoxicity of di(2-ethylhexyl) phthalate using mouse and human embryonic stem cell test models in vitro. 50. Zhonghua Yufang Yixue Zazhi 6 (7), 645–651 ([Article in Chinese]).
Marsee, K., Woodruff, T.J., Axelrad, D.A., et al., 2006. Estimated daily phthalate exposures in a population of mothers of male infants exhibiting reduced anogenital distance. Environ. Health Perspect. 114 (6), 805–809.
Pal, R., Mamidi, M.K., Das, A.K., Bhonde, R., 2011. Human embryonic stem cell proliferation and differentiation as parameters to evaluate developmental toxicity. J. Cell. Physiol. 226 (6), 1583–1595.
Patel, L., Pass, I., Coxon, P., Downes, C.P., Smith, S.A., Macphee, C.H., 2001. Tumor suppressor and anti-inflammatory actions of PPARgamma agonists are mediated via upregulation of PTEN. Curr. Biol. 11 (10), 764–768.
Ranstam, J., 2016. Multiple P-values and Bonferroni correction. Osteoarthritis Cartilage 24, 763–764.
Rowdhwal, S.S.S., Chen, J., 2018. Toxic effects of di-2-ethylhexyl phthalate: an overview. BioMed Res. Int. 1750368. https://doi.org/10.1155/2018/1750368.
Scholz, G., Spielman, H., 2000. Embryonic stem cell test (EST). INVITTOX 113, 1–33.
Schwartz, G.K., Shah, M.A., 2005. Targeting the cell cycle: a new approach to cancer therapy. J. Clin. Oncol. 23 (36), 9408–9421.
Singh, S., Li, S.S., 2011. Phthalates: toxicogenomics and inferred human diseases. Genomics 97 (3), 148–157.
Swan, S.H., 2008. Environmental phthalate exposure in relation to reproductive outcomes and other health endpoints in humans. Environ. Res. 108 (2), 177–184.
Ungrin, M.D., Joshi, C., Nica, A., et al., 2008. Reproducible, ultra high-throughput formation of multicellular organization from single cell suspension-derived human embryonic stem cell aggregates. PLoS One 3 (2), e1565.
Verano-Braga, T., Miethling-Graff, R., Wojdyla, K., 2014. Insights into the cellular response triggered by silver nanoparticles using quantitative proteomics. ACS Nano 8, 2161–2175.
Xu, Y., Cook, T.J., Knipp, G.T., 2006. Effects of di-(2-ethylhexyl)-phthalate (DEHP) and its metabolites on fatty acid homeostasis regulating proteins in rat placental HRP-1 trophoblast cells. Toxicol. Sci. 84 (2), 287–300.
Xu, Y., Agrawal, S., Cook, T.J., Knipp, G.T., 2007. Di-(2-ethylhexyl)-phthalate affects lipid profiling in fetal rat brain upon maternal exposure. Arch. Toxicol. 81 (1), 57–62.
Yousefi, B., Azimi, A., Majidinia, M., et al., 2017. Balaglitazone reverses P-glycoproteinmediated multidrug resistance via upregulation of PTEN in a PPARγ- dependent manner in leukemia cells. Tumor Biol. 39 (10) 1010428317716501.
Yu, G.Y., Cao, T., Ouyang, H.W., et al., 2013. Development of human embryonic stem cell model for toxicity evaluation. Beijing Da Xue Xue Bao 45 (1), 9–11.
Zhang, W., Shen, X.Y., Zhang, W.W., et al., 2017. Di-(2-ethylhexyl) phthalate could disrupt the insulin signaling pathway in liver of SD rats and L02 cells via PPARγ. Toxicol. Appl. Pharmacol. 316, 17–26.